Self-diffusion, mass transfer, and viscosity coefficients for a binary mixture in narrow slit-like pores

Yu. K. Tovbin and A. B. Rabinovich*

State Research Center of the Russian Federation "L. Ya. Karpov Institute of Physical Chemistry", 10 ul. Vorontsovo Pole, 103064 Moscow, Russian Federation. Fax: +7 (495) 975 2450. E-mail: tovbin@cc.nifhi.ac.ru

The concentration dependences of the dynamic characteristics of a binary mixture in narrow slit-shaped pores of different widths are considered. The local and mean partial self-diffusion, label transfer, mass transfer (mutual diffusion), and shear viscosity coefficients for binary mixtures of various compositions were calculated. The calculation was based on the lattice-gas model in the quasichemical approximation for spherical components with approximately the same size. The calculation of dynamic characteristics took into account collisions between the molecules that determine the direction of their motion. All the kinetic coefficients depend substantially on the mixture density, the direction of motion, and the distance to the pore wall. The effect of the pore width on the calculated dynamic characteristics is considered.

Key words: adsorption, narrow pores, mixture, self-diffusion coefficient, mass transfer coefficient, shear viscosity coefficient, lattice-gas model, quasichemical approximation.

The transport of molecules in porous solids plays an important role in catalytic, adsorption, and membrane processes.[1—6] In narrow (up to 10—15 nm) pores, the wall potential influences the aggregation state of the fluid and, correspondingly, the transport mechanisms.[7] In narrow pores, the transport characteristics of the adsobate change compared to those in the bulk phases.

Traditionally, the transport of molecules is described using mass, momentum, and energy transfer equations, well known in the thermodynamics of irreversible processes.[8—10] Assuming that the process is isothermal, one can restrict himself to the continuity equation and the mixture motion equation. The diffusion and shear viscosity coefficients are the most important dynamic characteristics. The theoretical calculation of these values over a broad range of degrees of filling (in the gaseous and liquid states) and temperature is hampered. Therefore, currently these dynamic characteristics of adsorbates are mainly calculated using molecular dynamics.[11—13] Recall also that the available experimental methods used to measure the self-diffusion coefficients even for pure components (NMR and particle labeling) give results that differ appreciably from the measurements of flow characteristics.[5,14] For mixtures, the situation is even more complicated. In particular, the concentration dependences of these coefficients for dense gases and liquids in narrow pores are unknown. Moreover, on passing from a one-component flow to the transport of mixtures, additional transfer coefficients should be introduced. The presence of a chemical potential gradient under nonequilibrium conditions gives rise to mass transfer coefficients. When the pressure is constant, these coefficients reflect the gradients of component concentrations, while for a constant mixture composition, this reflects the gradient of the overall pressure. One should also take into account the thermodiffusion transfer coefficients.[9,10] The concentration dependences of all these coefficients have not been studied. Similarly, the shear viscosity coefficient η is of greatest importance for the momentum transfer equation, and its concentration dependences in narrow pores have not been analyzed either.

This study involves a theoretical consideration of the concentration dependences of dynamic characteristics governing the transport of components of an adsorption mixture in narrow slit-shaped pores with different widths. The use is made of the lattice-gas model (LGM),[15] which takes into account the proper volume of atoms and interactions between the atoms in the quasichemical approximation. The LGM provides good agreement with molecular-dynamic calculations of the self-diffusion coefficient for one-component fluids, while requiring less time.[16,17] For narrow-pore systems, the model also provides phase diagrams of one-component fluids, which are in good agreement with the diagrams[18,19] and viscosity coefficients of one-component fluids[20,21] obtained by Monte Carlo and molecular dynamics methods.

This model allows one to find, using a single set of energetic parameters, self-consistent equilibrium characteristics of a vapor—liquid system and the molecular transfer coefficients in the bulk phase. The same parameters

Published in Russian in *Izvestiya Akademii Nauk. Seriya Khimicheskaya,* No. 8, pp. 1726—1735, August, 2005.

1066-5285/05/5408-1777

were used to calculate the partial and mean self-diffusion coefficients, mass transfer coefficients for variable chemical compositions and overall pressures of a binary mixture, and shear viscosity coefficients. For the sake of simplicity, we will restrict ourselves to the condition that components have a spherical shape and approximately the same size. Although this restriction is applicable only to isotope mixtures, it provides reliable results for many mixtures of molecules that do not differ much in size. Therefore, this is widely used for bulk solutions,[22,23] and the LGM itself is applied to mixtures of molecules with different size.[22,23] We consider only the case of a monodisperse system of slit-shaped pores. The equations for the adsorption isotherms of mixtures of spherical molecules with approximately the same size in a polydisperse system of slit-shaped pores were reported previously.[24]

Lattice-gas model and isotherm equations

In the LGM (see Refs 15 and 24), the volume of a slit-shaped pore V_p is split into H monoatomic layers with the linear size (width) λ, which are parallel to the pore wall, and each layer is split into units with a size similar to the particle volume $v_0 = \lambda^3$ to eliminate the double occupation of a unit (adsorption site or cell) with different molecules. Then $V_p = Nv_0$, where N is the number of sites in the system. The number of neighboring sites in the lattice structure is designated by z. Each site may accommodate only one particle: either a sort i molecule (if the center of mass of the molecule is located inside the site) or vacancy v. Different i correspond to different sorts of mixture components. The number of different states of occupation of any system site is designated by s; hence, the number of components is $s - 1$.

Usually, the concentration of molecules is defined as the number of these molecules N_i per site volume: $C_i = N_i/V_p$. In the lattice-gas model, the concentration of a fluid component is characterized by $\theta_i = N_i/N$, which is the ratio of the number of real particles of sort i in some volume to the maximum possible number of closely packed particles in the same volume. Then $\theta_i = C_i v_0$. The local density of particles i in a site with the number f will be designated by θ_f^i. The local densities are normalized in the following way: $\sum_{i=1}^{s-1}(\theta_f^i + \theta_f^v) = 1$. The average partial concentration of the fluid θ_i is determined through local concentrations: $\theta_i = \sum_{f=1}^{t} F_f \theta_f^i$, where F_f is the fraction of sites of type f ($1 \le f \le t$), t is the number of site types in the system, while the average total degrere of pore filling $\theta = \sum_{i=1}^{s-1}\theta_i$. The character $\{P\} \equiv P_1, \ldots, P_{s-1}$ stands for the whole set of all partial pressures of mixture components P_i, $1 \le i \le s - 1$.

Each site f is characterized by a specific interaction energy Q_f^i of sort i molecules with the walls and, hence, by a specific Henry constant a_f^i. In terms of this parameter, all lattice sites can be divided into groups with the same properties. If the walls of a slit-shaped pore are uniform, all sites of one layer are equivalent; therefore, the number f of the layer coincides with the number of site located therein. For an even number of monolayers, $t = H/2$, while for an odd number, $t = (H + 1)/2$. The local partial Henry constant is given by $a_f^i = a_f^{i0}\exp(\beta Q_f^i)$, where $\beta = (kT)^{-1}$, a_f^{i0} is the pre-exponent of the Henry constant, Q_f^i is the binding energy of molecule i in layer f with both walls, which is found as $Q_f^i = u_i(f) + u_i(H - f + 1)$ ($1 \le f \le t$), and the interaction potential between the molecule and the pore wall, $u_i(f) = \varepsilon_{si}[(\sigma_{si}/f)^9 - (\sigma_{si}/f)^3]$ is the Lennard-Jones potential averaged over the volume of the solid,[25] ε_{si} is the energy parameter of the interaction potential between component i and the adsorbent. Thus, the fraction of sites F_f in layer f equals $2/H$ for even H and odd H when $1 \le f \le t - 1$. Then $F_f = 1/H$ for $f = t$. The normalization condition for the sites of different types has the form $\sum_{f=1}^{t} F_f = 1$.

The average partial adsorption isotherms $\theta_i(\{P\})$ and local degrees of filling $\theta_f^i(\{P\})$ for spherical mixture components with roughly the same size on various adsorption sites will be calculated using the set of equations taking into account the energy heterogeneity of the lattice sites and the interactions of the molecules located at distance R between the coordination spheres:[15]

$$\theta_i(\{P\}) = \sum_{f=1}^{t} F_f \theta_f^i(\{P\}), \qquad (1)$$

$$a_f^i P_i = \theta_f^i \Lambda_f^i / \theta_f^v,$$

$$\Lambda_f^i = \prod_r \prod_g \left[S_{fg}^i(r)\right]^{z_{fg}(r)},$$

$$S_{fg}^i(r) = 1 + \sum_{j=1}^{s-1} [x_{fg}^{ij}(r) t_{fg}^{ij}(r)],$$

$$x_{fg}^{ij}(r) = \exp[-\beta\varepsilon_{fg}^{ij}(r)] - 1,$$

where $\beta = (kT)^{-1}$; the function Λ_f^i takes into account the intermolecular interactions in the quasichemical approximation; r is the number of the coordination sphere, $r \le R$; R is the radius of the interaction potential. The subscript g runs through all neighbors $z_f(r)$ of site f separated from it by distance r (radius of the coordination sphere), $z_{fg}(r)$ is the number of such neighbors in layer g, $\varepsilon_{fg}^{ij}(r)$ is a parameter of the lateral interaction of sort i molecules of layer f with sort j molecules of layer g at the distance of the r-th coordination sphere. The interactions with vacancies (i, j = v) are equal to zero.

The $t_{fg}^{ij}(r) = \theta_{fg}^{ij}(r)/\theta_f^i$, and $\theta_{fg}^{ij}(r)$ functions are defined by the following algebraic set of equations:

$$\theta_{fg}^{in}(r)\theta_{fg}^{vv}(r) = \theta_{fg}^{iv}(r)\theta_{fg}^{vn}(r)\exp[-\beta\varepsilon_{fg}^{in}(r)], \qquad (2)$$

$$\sum_{j=1}^{s} \theta_{fg}^{ij}(r) = \theta_f^i.$$

The equations (1) and (2) for a specified set of $\{\theta_i\}$ or $\{P_i\}$ values can be solved by the Newton iteration method with an error not exceeding 0.1%. This provides the possibility of calculating the equilibrium characteristics, the rate of thermal motion of molecules in a dense gas or a liquid, and all dynamic characteristics of the flow in narrow pores.

Equilibrium distributions of components in an argon—krypton mixture

The argon—krypton system in activated carbon was chosen for studying the concentration dependences of the dynamic characteristics. We assumed that the walls of the slit-shaped pores in activated carbon are formed by carbon atoms. The lateral interactions ε are determined using the Lennard-Jones potential $U_{ij} = 4\varepsilon_{ij}[(\sigma_{ij}/r)^{12} - (\sigma_{ij}/r)^6]$ for $r/\sigma_{ij} = 2^{1/6}$, which corresponds to a minimum of this potential. The molecular parameters of the mixture components are well-known: the argon atom has $Q_1^1 = 9.24\varepsilon_{ArAr}$ for $\varepsilon_{ArAr}/k_B = 119$ K, and the krypton atom has $Q_1^2 = 12.17\varepsilon_{ArAr}$ and $\varepsilon_{KrKr}/\varepsilon_{ArAr} = 1.37$ (~326 cal mol^{-1} or 163 K).[25,26] The interaction parameter between particles of different sorts was estimated as $\varepsilon_{12} = (\varepsilon_{11}\varepsilon_{22})^{1/2}$. For the argon—krypton system, the difference between the solid-sphere Lennard-Jones potential is rather small: $\sigma_{ArAr} = 0.3405$ nm and $\sigma_{KrKr} = 0.363$ nm.[25,26] For the sake of simplicity, the pore width was assumed to be commensurable with the lattice parameter $\lambda = 2^{1/6}\sigma$, where $\sigma = (\sigma_{ArAr} + \sigma_{KrKr})/2$.

The fluid structure was modeled by a lattice with 12 nearest neighboring sites. The pore width varied from 3 to 30 monolayers. The wall potential was taken into account up to distances at which the energy becomes lower than the thermal motion energy of the molecule, $Q_f^{Ar} \approx 0.1\varepsilon_{ArAr}$. All of the sites separated by more than four monolayers from the walls are considered to be equivalent. In order to rule out the appearance of two-phase regions, the calculations were restricted to isothermal conditions for $T = 1.5T^{crit}(Ar)$, where $T^{crit}(Ar)$ is the critical temperature of argon.

All expressions for the transfer coefficients are constructed with the assumption of insignificant deviations of the nonquilibrium distribution from the equilibrium one. Therefore, first of all, it is necessary to consider the equilibrium distribution of the components across the pore cross-section.

An idea of the equilibrium distributions of the argon and krypton atoms across a cross-section of the slit-shaped pore with the width $H = 10$ monolayers can be gained from Fig. 1, which shows the local partial degrees of filling by argon and krypton atoms in various monolayers for five compositions of the mixture $X_{Ar} = \theta_{Ar}/\theta$ at a constant overall density of the mixture θ inside the pore. Due to

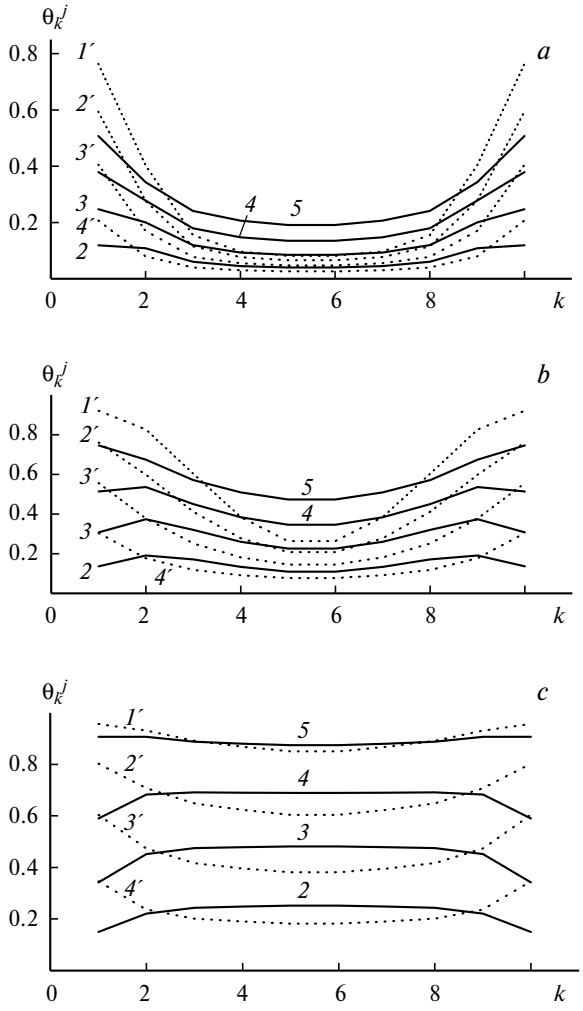

Fig. 1. Distributions of argon (full lines) and krypton (dotted lines, primed curve numbers) atoms during adsorption of an argon—krypton mixture in a slit-shaped pore for compositions with $X_{Ar} = 0$ (*1*), 1/4 (*2*), 1/2 (*3*), 3/4 (*4*), and 1 (*5*) for θ = 0.3 (*a*), 0.6 (*b*), and 0.9 (*c*); *k* are the monolayer numbers, θ_k^j are the local degrees of filling for mixture components.

the identity of the walls of the slit-shaped pore, the distribution curves of the mixture components across the pore section are symmetrical with respect to its center. Figure 1, *a* refers to the case of relatively low total degree of filling (θ = 0.3): both components are concentrated near the walls, while the central part of the pore is filled to a lesser extent. The krypton atoms are attracted more strongly than the argon atoms. Therefore, for pure krypton, the concentration of atoms in the surface layer is higher than for pure argon, while that in the pore center is lower. As the fraction of the first component X_{Ar} decreases, its concentration near the wall decreases, while that of the second component increases. The effect of the wall potential extends to three monolayers, its influence on the fourth and fifth monolayers is minor. All the curves

follow similar patterns and show the concentration minimum at the pore center.

The component distribution for the intermediate region ($\theta = 0.6$) is more complex (see Fig. 1, *b*). Krypton displaces argon from the first monolayer; therefore the curves for argon distribution across the cross-section pass through maxima, the argon atoms being concentrated in the second monolayer. In this case, too, the lowest concentrations of krypton atoms are found at the pore center, but they are higher in magnitude. In the case of a high degree of filling of the pore bulk ($\theta = 0.9$), the minimum concentrations of the krypton atoms are observed at the pore center at any composition (see Fig. 1, *c*). Pure argon is distributed across the surface almost uniformly. As the argon fraction in the mixture decreases, it is concentrated in the central region of the pore, because krypton is mainly located near the pore walls.

Thermal velocity of molecules

To describe the flows of mixtures in narrow pores, one should use a generalization of the proposed LGM,[15] which retains the same definition of the mutual diffusion coefficient for dense phases as for the gas phase. A detailed account of the LGM modification has been reported previously.[27] The essence is that for calculating the contribution of molecule *i* to the transport flow, it is necessary to take into account the sort of molecule *j* that collides with molecule *i*. This is necessary to describe the "source" of the forward motion of the molecule along the so-called ρ-scale. In all other respects, LGM equations[15] remain the same. The modification[27] retains the equilibrium characteristics of the system both in the bulk phase and in the pores, the allowance made for the inflience of lateral interactions on all the dynamic characteristics of molecules being described in self-consistence with the change of the equilibrium characteristics. This modification elucidates more precisely the role of particular collisions of the neighboring molecules *j* with the migrating molecule *i*. For this purpose, a neighboring site with subscript ξ is defined relative to site *f* in the so-called ρ-scale. Unit ξ accommodates molecule *j*, which determines the momentum and the jump direction of molecule *i* from site *f* to free site *g*. The site ξ is located on one straight line with sites *f* and *g* but on the other side of site *f*.

The jump velocity of molecule *i* by distance χ from site *f* to vacant site *g* can be expressed as follows:

$$U_{\xi fg}^{iv}(\chi) = \sum_{j=1}^{s-1} U_{\xi fg}^{(j)iv}(\chi), \qquad (3)$$

$$U_{\xi fg}^{(j)iv}(\chi) = K_{\xi fg}^{(j)iv}(\chi) V_{\xi fg}^{(j)iv}(\chi),$$

$$V_{\xi fg}^{(j)iv}(\chi) = \theta_{fg}^{iv}(\chi) \langle t_{f\xi}^{ij} \rangle \Lambda_{\xi fg}^{iv}(\chi),$$

$$\theta_{fg}^{iv}(\chi) = \theta_{fg(1)}^{iv}(1) \prod_{\psi} t_{\psi\psi+1}^{vv}(1),$$

$$\langle t_{f\xi}^{ij}(\rho) \rangle = t_{f\xi}^{ij}(\rho) \exp[\beta\delta\varepsilon_{f\xi}^{ij}(1.5\rho)]/\theta_f, \qquad (4)$$

$$\delta\varepsilon_{fh}^{ij}(r) = \varepsilon^{*}{}_{fh}^{ij}(r) - \varepsilon_{fh}^{ij}(r),$$

where the rate constant for jumps, $K_{\xi fg}^{(j)iv}(\chi) = (2\pi\mu_{ij}\beta)^{-1/2} \exp[-\beta E_{fg}^{iv}(\chi)]/\chi$, has the usual form except that the reduced mass μ_{ij} of the colliding molecules *i* and *j* is used instead of the mass of one molecule m_i; here $E_{fg}^{iv}(\chi)$ is the activation energy for a jump by distance χ in the action field of the pore wall potential (for sites remote from the pore walls, $E_{fg}^{iv}(\chi) = 0$). A molecule moving along the normal to the wall inside the pore acquires the momentum from the surface atoms; in this case, the rate constant for desorption contains the reduced mass μ_{iw}, where the subscript w refers to a wall atom (or group of atoms).[27] This distinguishes the rate constant for desorption from the rate constants for the migration of the molecule in the flow away from the walls, the adsorption, or surface migration on the wall. The relationship between the jump constants and the local Henry constants is described by the expressions $a_f^i K_{\xi fg}^{(j)iv}(\chi) = a_g^i K_{fg\xi}^{vi(j)}(\chi)$.

The concentration dependence of the rate of the migration of molecules is expressed by the co-factor $V_{\xi fg}^{(j)iv}(\chi)$. This includes the following three factors:

1. The probability $\theta_{fg}^{iv}(\chi)$ of existence of a free path from site *f* to site *g* with length χ that does not hit on other molecules.

2. The probability $\langle t_{f\xi}^{ij} \rangle$ that neighboring particle *j* is located in site ξ in the same straight line with sites *f* and *g* (in the ρ-scale), described by relation (4), where $\varepsilon^{*}{}_{fh}^{ij}(r)$ is the interaction parameter of the active complex for the migration of molecule *i* from site *f* with neighboring molecule *j*, which exists in the ground state in site *h* at distance *r*, $r \le R$. The coefficient of 1.5 found in the argument of the energy parameters, $r = 1.5\rho$, implies the saddle point coordinate with respect to site ξ (for ideal gas, $\rho > R$ and $\langle t_{f\xi}^{ij} \rangle = x_i$).

3. The function $\Lambda_{\xi fg}^{iv}(\chi)$, which takes into account the influence of lateral interactions of the neighboring molecules arranged around this path on the probability of jump along the path. In the quasichemical approximation, it is expressed as follows:

$$\Lambda_{\xi fg}^{iv}(\chi) = \prod_{r=1}^{R} \prod_{\omega_r=1}^{\pi_r} \prod_{h \in m^{*}(\omega_r)} \sum_{k=1}^{v} t_{fgh}^{ivk}(\omega_r) E_{fgh}^{ivk}(\omega_r), \qquad (5)$$

$$t_{fgh}^{ivk}(\omega_r) = \theta_{fh}^{ik}(r_1) \theta_{gh}^{vk}(r_2) / (\theta_f^i \theta_g^v \theta_h^k),$$

$$E_{fgh}^{ivk}(\omega_r) = \exp\{\beta[\delta\varepsilon_{fh}^{ik}(r_1) + \delta\varepsilon_{gh}^{vk}(r_2)]\}.$$

A specified jump distance χ corresponds to the distance from site *h* to site *f*, equal to r_1, and that to site *g*,

equal to r_2. The sites h belong to the set $m(\omega_r)$ with fixed distance r and angle ω_r. The ω_r angle describes the position of site h; this is the angle formed by the line connecting a pair of "central" sites fg and the line connecting site h with the midpoint of the segment fg. The set $m(\omega_r)$ includes the sites located at the distance r from a central site (f or g); $m^*(\omega_r) = m(\omega_r) - 1$, which implies the lack of a factor at $h = \xi$ in the right-hand part of Eq. (5).

Dynamic characteristics[27]

Label transfer coefficients. The local mass transfer coefficient for a particular component, which characterizes redistribution or thermal motion of molecule i ($1 \le i \le s-1$) between neighboring sites f and g, situated in the neighboring planes at distance χ under equilibrium conditions, is the simplest characteristics of the molecular transport in the mixtures.

For a "labeled" molecule of sort i, the expression for the local partial label transfer coefficient has the form

$$D_{\xi fg}^{*i}(\chi) = z_{fg}^{*}(\chi)\chi^2 U_{\xi fg}^{iv}(\chi)/\theta_f^i, \qquad (6)$$

where $z_{fg}^{*}(\chi)$ is the number of possible jumps to neighboring sites g by distance χ for each site f. The label transfer coefficient for each component depends appreciably on the local distributions of the components across the pore cross-section and on the direction of the motion. It also depends on the total local density of the system and intermolecular interactions.

Mean label transfer coefficient describes the label movement along the pore axis. For a slit-shaped pore, the following expression for the mean transfer coefficient of label i ($1 \le i \le s-1$), obtained by averaging over all sites situated in the pore cross-section, is valid:

$$D_i^* = \sum_{\chi} \chi^2 \sum_{f=1}^{t} F_f \sum_{g=1}^{t} \left\{ \left[z_{fg}^{*}(\chi) U_{\xi fg}^{iv}(\chi)/\theta_f^i \right] \frac{d\theta_f^{*i}}{d\theta_i^*} \right\}, \qquad (7)$$

where $z_{fg}^{*}(\chi)$ is the number of bonds along which the jumps by distance χ take place from a site in layer f to neighboring sites in layer g, $d\theta_f^{*i}/d\theta_i^* = d\theta_f^i/d\theta_i$.

Mutual diffusion coefficient. The local mutual diffusion coefficient for a binary mixture at constant pressure and temperature is given by

$$D_{\xi fg}^{1,2}(\chi) = x_2[D_{\xi fg}^{11}(\chi) - D_{\xi fg}^{12}(\chi)] + x_1[D_{\xi fg}^{22}(\chi) - D_{\xi fg}^{21}(\chi)], \qquad (8)$$

where the addends have the form

$$D_{\xi fg}^{ik}(\chi) = \sum_{j=1}^{s-1} z_{fg}^{*}(\chi)\chi^2 U_{\xi fg}^{(j)iv}(\chi) \times \frac{d\{\ln[Y_{fg}^{i}(\chi) Y_{f\xi}^{ij}(\rho) a_f^{i*} p_i]\}}{dx_k} / (\theta_f v_0), \qquad (9)$$

$$Y_{fg}^{i}(\chi) = \theta_{fg}^{vv}(\chi)/[t_{fg}^{iv}(\chi) t_{gf}^{iv}(\chi)],$$

$$Y_{fg\xi}^{ij}(\rho) = \langle t_{f\xi}^{ij}(\rho) \rangle / S_{f\xi}^{i}(\rho).$$

Here a_f^{i*} is a part of the local Henry constant independent of the density (all the density-dependent contributions to the Henry constant (a_f^i/a_f^{i*}) occur in the right-hand part Eq. (9), together with the imperfection function Λ_f^i). For macroscopic distances $Y_{fg}^{i}(\chi) = 1$, relation (9) for the mean mass transfer coefficients of molecules i on the change in the mole fractions x_j is also transformed into the known expression[28,29] that relates the mass transfer coefficient to the gradient of the chemical potential of component i.

The mutual diffusion coefficient averaged over the pore cross-section is calculated by the relation analogous to Eq. (7):

$$D_{1,2} = \sum_{\chi} \sum_{q=1}^{t} F_q \sum_{p=1}^{t} D_{\xi qp}^{1,2}(\chi). \qquad (10)$$

Shear viscosity coefficient. The local viscosity coefficient η_{fg} upon the shear of a mixture of molecules with a commensurable size and a spherical shape in site g relative to site f (here $\chi = 1$; therefore, this character is omitted) is equal to

$$\eta_{fg} = \left[\sum_{i=1}^{s-1} x_j \left(\eta_{fg}^{j} \right)^{-1} \right]^{-1}, \qquad (11)$$

$$\eta_{fg}^{j} = \theta_f^j / U_{\xi fg}^{iv}, \qquad x_f^i = \theta_f^i/\theta_f, \qquad \theta_f = \sum_{i=1}^{s-1} \theta_f^i,$$

where x_f^i is the mole fraction of component j in site f, θ_f is the total filling of site f, and $U_{\xi fg}^{iv}(\chi = 1)$ can be found from Eq. (3).

Bulk phase and calculation conditions

To determine the transfer coefficients, one can use relations (3)—(5) for the average relative velocity of thermal motion of molecule i taking into account their collisions with all of the neighboring molecules. For small degrees of filling corresponding to the gas phase volume, no contributions of lateral interactions are involved, and Eq. (3) will take the form $U_{\xi fg}^{iv}(\chi) = \sum_{j=1}^{s-1} K_{\xi fg}^{(j)iv}(\chi) x_j \theta_f (1 - \theta_g)^{\chi}$. The mean relative velocity w_{fg}^{i} of component i is expressed in terms of the jump velocity as $w_{fg}^{i} = \chi U_{\xi fg}^{iv}(\chi)/\theta_f^i$. Under these conditions, relations (3)—(5) are transformed into new equations for a rarefied gas. In particular, they give expressions for the mutual diffusion coefficient,[27] which are in line with the strict kinetic theory.[6,9,30]

The normalized concentration dependences of the mutual diffusion coefficient in an argon—krypton binary gas

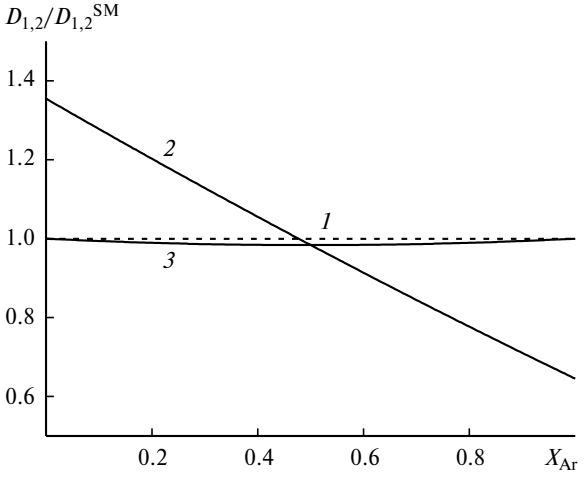

Fig. 2. Normalized concentration dependences of the mutual diffusion coefficient in an argon—krypton binary mixture upon the variation of the argon mole fraction calculated using the Stefan—Maxwell[30] (*1*) and Meyer[30] (*2*) formulas and using modified LGM [27] (*3*). The normalization was done to the $D_{1,2}^{SM}$ value calculated for the same mixture using the Stefan—Maxwell formula.[30]

mixture for the change on the argon mole fraction are shown in Fig. 2. The results of calculation show that the LGM modification[27] markedly changes the pattern of dependence of the mutual diffusion coefficient for a binary mixture on the mole fraction of the light component (curve *3*) with respect to that calculated from the Meyer formula[30] (curve *2*). The greatest difference between the results obtained using relations (8) and (9) of the new modified model and the results of an analogous calculation using the Stefan—Maxwell formula[30] (curve *1*) is only 1.2%.

Dense mixtures were studied using the same molecular parameters as were used to construct the equilibrium density profiles in Fig. 1. For calculation of the jump velocity, the dimensionless parameter $\alpha = \varepsilon^*/\varepsilon = \varepsilon^*_{fh}{}^{ij}(r)/\varepsilon_{fh}{}^{ij}(r)$ was additionally used. Its magnitude was found from comparison with experimental data on the argon shear viscosity η in the bulk phase.[31] According to the experiment,[31] an increase in the argon density θ from a rarefied gas to a value of about 0.6 entails an almost twofold increase in η. The calculation carried out for a lattice structure with $z = 12$ showed that $\alpha \sim 0.55$ (Fig. 3, *a*, curve *6*).

The parameter α is fairly sensitive to the molecular parameters of the model. Previously,[32] a similar satisfactory agreement with the experiment was attained for a lattice with the number of the nearest neighbors $z = 6$ for $\alpha = 0.85$. However, in this case, apart from a different structural factor, the traditional version of LGM was used, which does not make allowance explicitly for the collisions with neighboring molecules.[15,33] The key distinction of the relations used[15,33] from formulas (3)—(5) lies in a different expression for imperfection function (5). The imperfection functions $\Lambda_{fg}{}^{iv}(\chi)$ are derived from functions $\Lambda_{\xi fg}{}^{iv}(\chi)$ by averaging over all occupation states of the site ξ; therefore, this subscript is missing from the former expressions. These particular relations in the quasichemical approximation have been repeatedly described previously;[15,33] therefore, we do not repeat them here.

The influence of the shear velocity model used on the concentration dependences of the shear viscosity coefficient over a broad range of densities of the argon—krypton mixture is illustrated in Fig. 3. The full lines show the plots calculated from relations (3)—(5) and (11), while

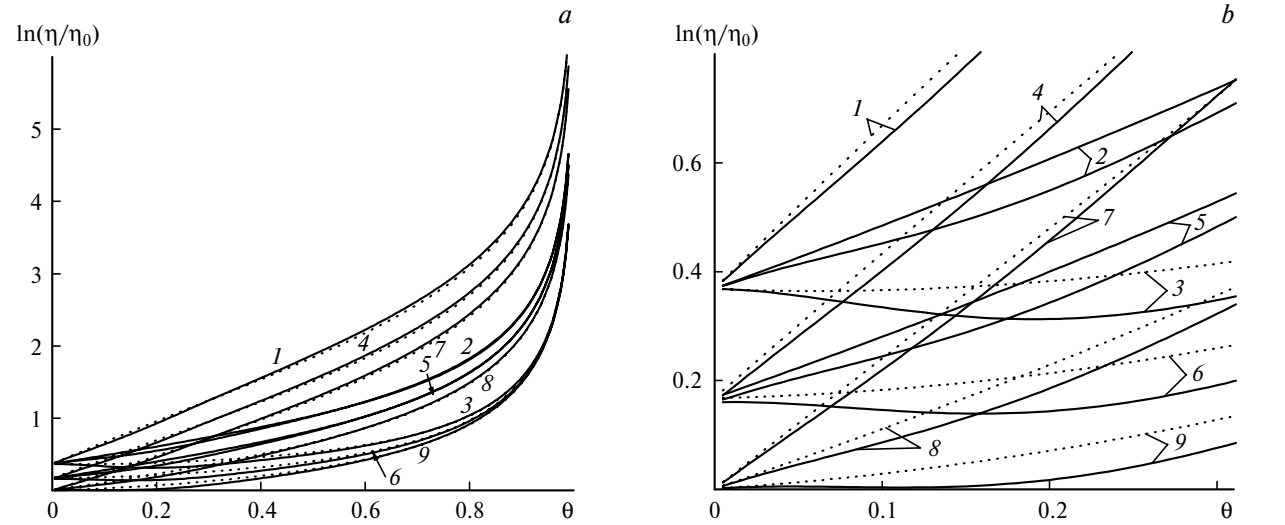

Fig. 3. Comparison of the concentration dependences of the shear viscosity coefficient calculated for a bulk phase for $T = 1.5T^{crit}(Ar)$, $\alpha = \varepsilon_{ij}^*/\varepsilon_{ij} = 0.3$ (*1—3*), 0.55 (*4—6*), and 0.7 (*7—9*) and $X_{Ar} = 1.0$ (*3*, *6*, *9*), 0.5 (*2*, *5*, *8*), and 0 (*1*, *4*, *7*): full range of densities of an argon—krypton mixture (*a*), low densities of the mixture (*b*).

dashed lines correspond to the curves constructed using the previously reported expressions[33] (note that an experiment[32] with pure argon for a structure with $z = 12$ gives $\alpha \sim 1.0$). At low degrees of filling, the old and new expressions yield markedly dissimilar curves. For clarity, the density region below $\theta \sim 0.3$ is shown in Fig. 3, *b* on a larger scale. The main rules of variation of the viscosity coefficient following an increase in the density of the mixture are similar in the two models; for $\theta > 0.4$, both models give roughly the same values (see Fig. 3, *a*).

In what follows, all the dynamic characteristics are normalized to the corresponding coefficients for argon in a rarefied gas phase.

Concentration dependences of the dynamic characteristics in the slits

When calculating the dynamic characteristics for the pure components and for the label transfer in the mixture, the following values were taken for molecular parameters: $H = 10$, $T = 1.5T^{crit}$, $R = 1$, $\alpha = 0.55$, $\alpha_{11} = E_{11}^{iv}(1)/Q_1^i = 1/3$ (this α_{11} value corresponds to the relatively low activation barrier to the surface jump), $Q_1 = 9.24\ \varepsilon_{ArAr}$.

Label transfer coefficients. Figure 4 shows the local concentration dependences of the label transfer coefficients for the argon and krypton atoms, which depend on the distance to the pore walls and migration direction, and the mean values for the partial label transfer coefficients. Curves *1*—*8* are the concentration curves that refer to all site pairs *fg*, where $g = f, f\pm1$. The mixture movement occurs within layer f for $g = f$ and along the normal to the surface of the slit-shaped pore for $g = f\pm1$. For $g = f + 1$, the motion is directed toward the pore center, which implies, for the wall attraction potential, a decrease in the binding energy to the wall following an increase in the layer number. This motion involves overcoming the activation barrier of the wall potential ($Q_f^i - Q_{f-1}^i$). Conversely, for $g = f - 1$, motion does not require overcoming the activation barrier of molecule *i* in the neighboring layers.

The partial label transfer coefficients for both components decrease as the sites of each type are being filled. On increasing pressure, the local coefficients referred to the surface monolayer are the first to decrease, while those referring to the central region are the last to decrease. The mean values for the label transfer coefficients (curves *9*) change nonmonotonically. They have a maximum corresponding to filling of the surface monolayer; after its completion, filling of the second monolayer starts. In this situation, migration in the second monolayer is rather

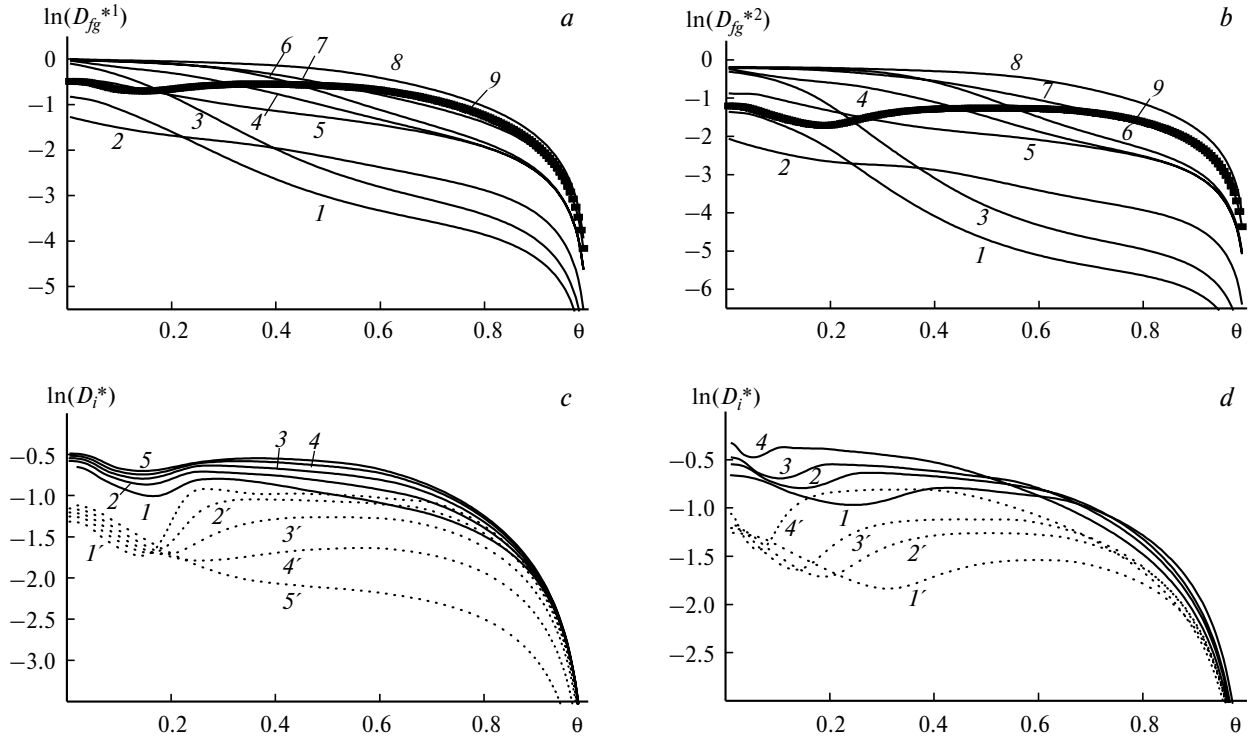

Fig. 4. Concentration dependences of the label transfer coefficients for argon (full lines) and krypton (dotted lines) atoms in their mixture at $H = 10$, $T = 1.5T^{crit}$, $R = 1$, $\alpha = 0.5$, $\alpha_{11} = 1/3$, $Q_1^{Ar} = 9.24\varepsilon$; the local coefficients for pairs of neighboring sites are given for layers *fg* = 11 (*1*), 12 (*2*), 21 (*3*), 22 (*4*), 23 (*5*), 32 (*6*), 33 (*7*), 55 (*8*), mean D_i^* value for $X_{Ar} = 0.5$ (*9*); (*a*, *b*) labels for argon and krypton, respectively; (*c*) D_i^* values for $X_{Ar} = 0.005$ (*1*), 1/4 (*2*), 1/2 (*3*), 3/4 (*4*), and 0.995 (*5*), (*d*) for $X_{Ar} = 0.5$ and pores with the width $H = 6$ (*1*), 10 (*2*), 14 (*3*), 30 (*4*).

fast. As the pore volume is being filled, the fraction of vacant sites decreases and all the label transfer coefficients descend.

The average D_i^* values for different mixture compositions are presented in Fig. 4, *c*. As the krypton fraction decreases and the argon fraction increases, the initial values for the argon and krypton label transfer coefficients increase, as their fraction in the surface monolayer changes. It can be see how krypton displaces argon into the central part of the pore, because krypton is adsorbed more strongly by the pore surface.

The concentration dependences of the average mass transfer coefficients for the argon and krypton atoms for pores of different width are shown in Fig. 4, *d*. As H increases, the contribution of the central part of the pore becomes more pronounced; therefore, the region of nonmonotonic variation of the coefficients shifts to lower densities, and the whole curve shifts (after the minimum) toward the analogous curve for the bulk phase.

Mutual diffusion coefficient. The concentration curves for the mutual diffusion coefficient in slit-shaped pores are shown in Fig. 5. The general pattern of the curves shown in Fig. 5, *a* resembles that of the concentration curves of the label transfer coefficients of both components considered above. They exhibit the same sharp anisotropy with respect to the direction of the local transfer and a substantial dependence on the distance to the wall. However, quantitative differences are obvious. Figure 5, *b* shows the variation of the mean mutual diffusion coefficient for different molar compositions of the mixture in a 10 monolayer-wide slit-shaped pore. Unlike the label transfer coefficient, the mean value of the mutual diffusion coefficient depends little on the mole fractions of the components in a binary mixture; therefore, all curves virtually run into one. This is similar to the well-known variation of the mutual diffusion coefficient in gases. The effect of the mole fraction is shown in more detail in the inset of Fig. 5, *b*. The *y*-axis gives the normalized values of the mutual diffusion coefficient for five X_{Ar}, which were normalized to the same coefficient at $X_{Ar} \to 0$. The inset has the same meaning as that in Fig. 2, although it refers to different total degrees of pore filling. For comparison, curve *5* is shown, which refers to a bulk gas phase far from the region of influence of the pore walls. The scale of variation along the *y*-axis indicates that the change in the mean mutual diffusion coefficient is relatively small. However, in the general case, the behavior of $D_{1,2}(X_{Ar})$ upon the variation of the total degree of pore filling is not monotonic, due to the nonmonotonic influence of the wall potential.

Shear viscosity coefficient. The viscosity coefficients were calculated using the same molecular parameters as were used to estimate the diffusion coefficients (Fig. 6). The components of the shear viscosity tensor in a 10 monolayer-wide slit-shaped pore for equal amounts of

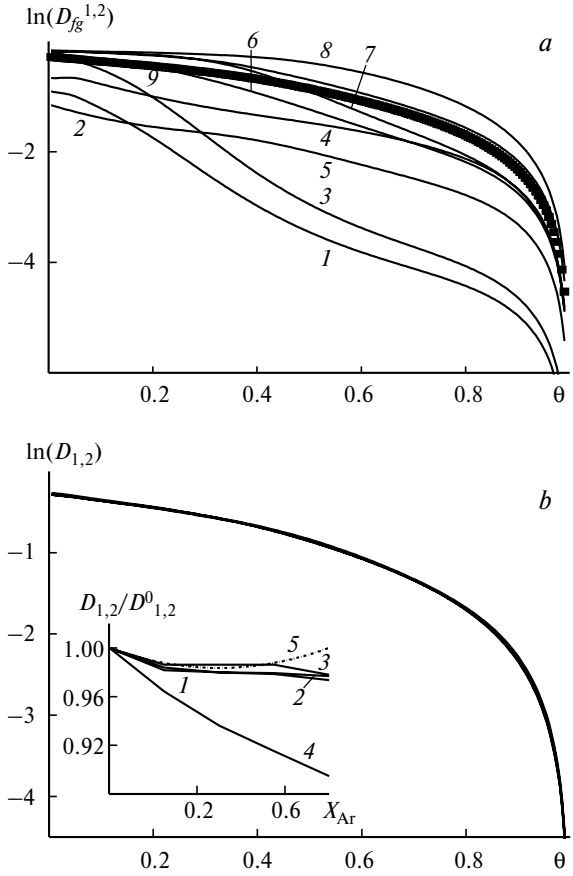

Fig. 5. Concentration dependences of the mutual diffusion coefficients (*a*) and the mean mutual diffusion coefficient (*b*); the local coefficients are given for various pairs of sites *fg* for the parameters indicated in Fig. 4, *a*; variation of the mixture composition in a pore for the values of parameters indicated in Fig. 4, *c*. The inset shows the normalized curves corresponding to Fig. 5, *b* calculated for a pore coverage of θ = 0.005 (*1*), 0.50 (*2*), 0.75 (*3*), 0.99 (*4*).

argon and krypton are shown in Fig. 6, *a*. As in the above examples, the initial local shear viscosity coefficients are determined by the wall surface potential. The motion along the surface layer involves overcoming the surface potential barrier, which is lower than the "desorption" value ($Q_2^i - Q_1^i$); therefore, for zero values, $\eta_{11}(0) < \eta_{12}(0)$. The $\eta_{12}(0)$ value is the greatest, as it refers the most pronounced change in the surface wall potential. (The same potential determines the relationships $\eta_{ff}(0) < \eta_{ff+1}(0)$ in the region of its action.) As the degree of pore filling increases, the first layer is the first to be filled; this determines the fast growth of $\eta_{11}(\theta)$, which exceeds $\eta_{12}(\theta)$ for filling degrees exceeding one monolayer (the sites of the second monolayer are blocked and the attraction of the surrounding molecules becomes more pronounced).

The variation of the mixture composition X_{Ar} is shown in Fig. 6, *b* for three layers, f = 1, 2, and 5. The most pronounced influence of the composition is followed for

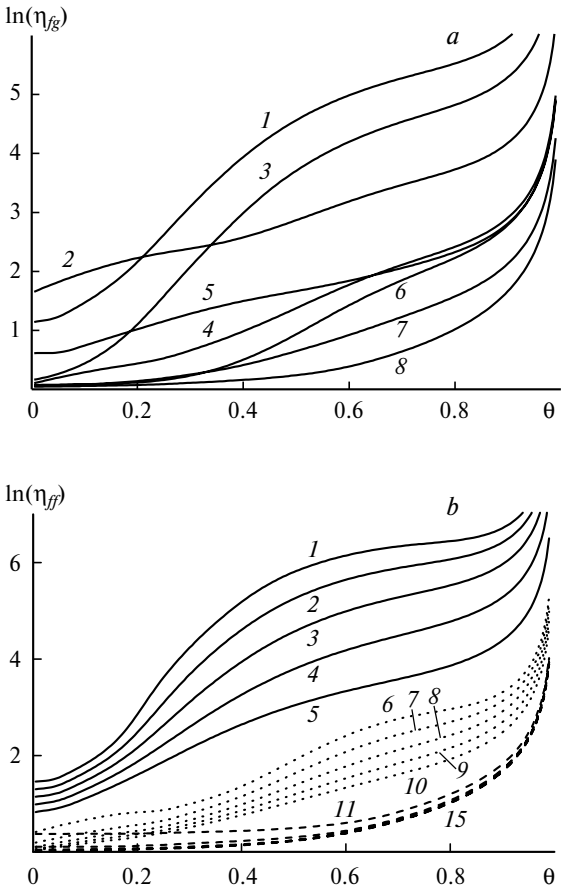

Fig. 6. Concentration dependences of local shear viscosity coefficients of an argon—krypton mixture; calculation conditions are similar to those used in Fig. 4; (*a*) local curves for $X_{Ar} = 0.5$ correspond to pairs of neighboring sites in layers *fg* = 11 (*1*), 12 (*2*), 21 (*3*), 22 (*4*), 23 (*5*), 32 (*6*), 33 (*7*), 55 (*8*); (*b*) coefficients η_{ff} (*f* = 1, 2 и 5) for the compositions $\gamma = 0$ (*1*, *6*, *11*), 1/4 (*2*, *7*, *12*), 1/2 (*3*, *8*, *13*), 3/4 (*4*, *9*, *14*), and 1.0 (*5*, *10*, *15*).

the surface layer, while the least pronounced one is found for the central layers: the η_{55} curves nearly merge into a line.

* * *

Thus, the dynamic characteristics of the mixture components depend appreciably on the anisotropic distribution of the molecules across the cross-section of the slit-shaped pore. The transfer coefficients change most sharply near the pore walls due to the most pronounced influence of the surface potential. At the pore center, these coefficients depend to a lesser extent on the contribution of the wall potential. An important role is played by the total concentration of the mixture of molecules. The denser the system, the lower the migration velocity and all the related mass transfer coefficients; conversely, the viscosity coefficient substantially increases.

For the transport of dense gases that are efficiently adsorbed by pore walls (for example, in activated carbons), an important role is played by sliding effects of the dense fluid. These effects have been usually considered only for rarefied gases. In dense adsorbates, the sliding effect is due to the surface mobility of the molecules rather than to the mirror reflection from the walls, as in the case of rarefied gases.

The traditional assumptions concerning the invariability of the self-diffusion[1,4] and shear viscosity[2] coefficients are not correct in the general case. When analyzing experimental data, one should take into account rather pronounced concentration dependence of the partial dynamic characteristics of an adsorbate mixture in narrow pores cased by both the effect of the pore wall potential and their intermolecular interactions. The molar composition of the mixture and the nature of intermolecular interactions of the components with the pore wall and with the other components determine the degree of component separation in each pore cross-section, which results in substantial nonlinear effects for the transfer coefficients upon the change of the overall density of the mixture.

This work was financially supported by the Russian Foundation for Basic Research (Project No. 03-03-32072).

References

1. D. P. Timofeev, *Kinetika adsorbtsii* [*Adsorbtion Kinetics*], Akad. Nauk SSSR, Moscow, 1962, 252 pp. (in Russian).
2. L. I. Kheifets and A. V. Neimark, *Mnogofaznye protsessy v poristykh sredakh* [*Multiphase Processes in Porous Media*], Khimiya, Moscow, 1982, 320 pp. (in Russian).
3. C. N. Satterfield, *Mass Transfer in Heterogeneous Catalysis*, MIT Press, Cambridge (Mass.), 1970.
4. D. M. Ruthven, *Principles of Adsorption and Adsorption Processe*, J. Wiley and Sons, New York, 1984.
5. *Adsorbtsiya v mikroporakh* [*Adsorption in Micropores*], Eds M. M. Dubinin and V. V. Serpinsky, Nauka, Moscow, 1983, p. 114 (in Russian).
6. E. A. Mason and A. P. Malinauskas, *Gas Transport in Porous Media: The Dusty-Gas Model*, Elsevier, Amsterdam, 1983.
7. Yu. K. Tovbin, *Mater. konf., posvyashchennoi 100-letiyu M. M. Dubinina* [*Proc. Conf. Dedicated to the 100th Anniv. Acad. M. M. Dubinin*], In-t Fiz. Khim. RAN, Moscow, 2001, 27 (in Russian).
8. L. D. Landau and E. M. Livshits, *Teoreticheskaya fizika, VI. Gidrodinamika* [*Theoretical Physics, VI. Hydrodynamics*], Nauka, Moscow, 1986, 733 pp. (in Russian).
9. R. B. Bird, W. E. Steawart, and E. N. Lightfoot, *Transport Phenomena*, J. Wiley, New York—London, 1965.
10. S. R. de Groot and P. Mazur, *Non-Equilibrium Thermodynamics*, North-Holland Publ. Company, Amsterdam, 1962.
11. B. D. Todd and D. J. Evans, *J. Chem. Phys.*, 1995, **103**, 9804.
12. J. M. D. MacElroy, *J. Chem. Phys.*, 1994, **101**, 5274.

13. E. Akhmatskaya, B. D. Todd, P. J. Davis, D. J. Evans, K. E. Gubbins, and L. A. Pozhar, *J. Chem. Phys.*, 1997, **106**, 4684.
14. R. Sh. Vartapetyan, A. M. Voloshchuk, and I. Kerger, *Materialy VIII Mezhdunar. konf. "Teoriya i praktika adsorbtsionnykh protsessov"* [*Proc. VIII Int. Conf. "Theory and Practice Adsorbtion Processes"*], In-t Fiz. Khim. RAN, Moscow, 1997, 63 (in Russian).
15. Yu. K. Tovbin, *Theory of Physical Chemistry Processes at a Gas—Solid Surface Processes*, CRC Press, Boca Raton (Fl), 1991.
16. M. A. Mazo, A. B. Rabinovich, and Yu. K. Tovbin, *Zh. Fiz. Khim.*, 2003, **77**, 2053 [*Russ. J. Phys. Chem.*, 2003, **77**, No. 11 (Engl. Transl.)].
17. M. A. Mazo, A. B. Rabinovich, and Yu. K. Tovbin, *Khim. Fizika* [*Chem. Physics*], 2004, **23**, No. 6, 47 (in Russian).
18. E. V. Votyakov, Yu. K. Tovbin, J. M. D. MacElroy, and A. Roche, *Langmuir*, 1999, **15**, 5713.
19. A. Vishnyakov, E. M. Piotrovskaya, E. N. Brodskaya, E. V. Votyakov, and Yu. K. Tovbin, *Zh. Fiz. Khim.*, 2000, **74**, 221 [*Russ. J. Phys. Chem.*, 2000, **74** (Engl. Transl.)].
20. Yu. K. Tovbin and N. F. Vasyutkin, *Zh. Fiz. Khim.*, 2002, **76**, 319 [*Russ. J. Phys. Chem.*, 2002, **76** (Engl. Transl.)].
21. Yu. K. Tovbin, E. E. Gvozdeva, and D. V. Eremich, *Zh. Fiz. Khim.*, 2003, **77**, 878 [*Russ. J. Phys. Chem.*, 2003, **77** (Engl. Transl.)].
22. I. R. Prigozhin, *Moleculyarnye teorii rastvorov* [*Molecular Theories of Solutions*], Khimiya, Moscow, 1987, 450 pp. (in Russian).
23. N. A. Smirnova, *Moleculyarnaya teoriya rastvorov* [*Molecular Theory of Solutions*], Khimiya, Leningrad, 1987, 360 pp. (in Russian).
24. Yu. K. Tovbin, *Izv. Akad. Nauk, Ser. Khim.*, 2003, 827 [*Russ. Chem. Bull., Int. Ed.*, 2003, **52**, 869].
25. W. A. Steele, *The Interactions of Gases with Solid Surfaces*, Pergamon, New York, 1974.
26. S. Sokolowski and J. Fischer, *Mol. Phys.*, 1990, **71**, 393.
27. Yu. K. Tovbin, *Izv. Akad. Nauk., Ser. Khim.*, 2005, 1717 [*Russ. Chem. Bull., Int. Ed.*, 2005, **54**, 1768].
28. K. P. Gurov, B. A. Kartashkin, and E. Yu. Ugaste, *Vzaimnaya diffuziya v mnogofaznykh metallicheskikh sistemakh* [*Mutual Diffusion in Many-Phase Metallic Systems*], Nauka, Moscow, 1981, 352 pp. (in Russian).
29. B. S. Bokshtein, S. Z. Bokshtein, and A. A. Zhukhovitskii, *Termodinamika i kinetika diffuzii v tverdykh telakh* [*Thermodynamics and Kinetics of Diffusion in Solids*], Metallurgiya, Moscow, 1976, 280 pp. (in Russian).
30. E. A. Moelwyn-Hughes, *Physical Chemistry*, Pergamon Press, London—New York—Paris, 1961.
31. I. A. Sokolova, *Obzory po teplofizicheskim svoistvam veshchestv* [*Reviews on Thermophysical Properties of Substances*], Izd-vo ITV RAN, Moscow, 1992, No. 2 (94), 36 (in Russian).
32. B. V. Egorov, V. N. Komarov, Yu. E. Markachev, and Yu. K. Tovbin, *Zh. Fiz. Khim.*, 2000, **74**, 882 [*Russ. J. Phys. Chem.*, 2000, **74** (Engl. Transl.)].
33. Yu. K. Tovbin, *Khim. Fizika* [*Chem. Physics*], 2004, **23**, No. 12, 82 (in Russian).

Received December 22, 2004